

Computing Multistatic Passive Radar CFAR Thresholds from Surveillance-Only Data

Konstanty S. Bialkowski I. Vaughan L. Clarkson
School of Information Technology and Electrical Engineering,
The University of Queensland, Qld, 4072, Australia

Abstract—A method inspired by Generalised Canonical Correlation (GCC) has been proposed as a detection statistic for multistatic passive radar when a noise-free reference signal is unavailable [1]. The GCC statistic can be expressed as the largest eigenvalue of the Gram matrix of the received signals. It is derived from a suitably formulated generalised likelihood ratio test (GLRT). The Gram matrix is drawn from a Wishart distribution: a central Wishart distribution in the target-absent case and a non-central Wishart distribution when the target is present. Numerical computation using the eigenvalue distribution is fraught with difficulties [2]. Exact theoretical expressions involve ratios of products of factorials which soon defeat attempts at straightforward implementation in double-precision floating point. On the other hand, standard approximations, such as the Tracy-Widom distribution [3], are inaccurate when a low false-alarm rate is required.

In this paper, we present a new method to accurately compute probabilities using standard double-precision floating-point arithmetic. This allows practical application of the GCC statistic to CFAR detection in passive radar scenarios where the number of samples is large (10^4 – 10^7), and the number of receivers is small (2–5).

Index Terms—Passive radar, signal detection, double precision

I. INTRODUCTION

In multistatic passive radar, multiple transmitters and/or receivers are used to locate targets in the environment. Unlike typical radar, passive radar uses existing transmitters in the environment, which makes the radar system a passive system [4], [5]. The intended purpose of these transmitters is not necessarily for radar, but for some other service such as telecommunication or geolocation. Hence, they are termed *illuminators of opportunity* [6].

Illuminators of opportunity, to be useful for passive radar, should, like any radar illuminator, have a high transmission power to provide adequate range and a ‘thumb-tack-like’ waveform ambiguity function to resolve closely spaced targets. The growing interest in passive radar can be explained at least in part by the proliferation of high-quality illuminators, including terrestrial and satellite digital TV, radio and cellular data services.

A passive radar has several benefits over an active radar. It emits no radiation of its own, so it can be operated covertly. Without the need of its own high-power transmitter, passive radar can be small and light. Targets which optimise their radar cross-section (RCS) against monostatic radar may have higher RCS in the multistatic geometry of a passive radar network.

The benefits of multistatic passive radar come at the cost of an increased detection complexity. Not knowing the transmitted signal means the usual detection techniques used for monostatic radar cannot be used. Several methods have been proposed for passive multistatic detection, such as the subspace projection method [7], the sample covariance method [8], generalised coherence [9], [10] and a method inspired by generalised canonical correlation, which we refer to simply as GCC [1].

Here, we analyse GCC, as proposed by the present authors with Howard in [1]. The detector is formed as a generalized likelihood ratio test (GLRT) with one hypothesis being that a target is present (\mathcal{H}_1), and the other that the target is absent (\mathcal{H}_0). The GLRT reduces to calculation of the largest eigenvalue of the Gram matrix constructed by stacking together the received signal vectors. We focus on the case of a single transmitter and M receivers. We let L be the number of received (complex-valued) samples in each received signal vector. Usually, $L \gg M$. The Gram matrix is an $M \times M$ matrix. Under the null (target-absent) hypothesis, the Gram matrix can be viewed as a scatter matrix drawn from a complex, central Wishart distribution.

The problem lies in the numerical computation of thresholds. If the exact expression of Kang & Alouini [11] is directly transcribed for computer calculation, it can only be computed feasibly when both L and M are small. These expressions involve ratios of products of factorials that soon overwhelm the capacity of double-precision floating-point numbers. In its application to calculation of thresholds for passive radar [2], Hack *et al.* note that “direct calculation...was infeasible for... $L \geq 10$ without variable precision arithmetic.” Even then, the threshold was only “successfully calculating...for $L \leq 100$ when $[M] \leq 6$.”

On the other hand, if L and M are large, then the Tracy-Widom (TW) distribution [3] becomes an accurate approximation of the distribution of the largest eigenvalue. For fixed values of L and M , the fidelity of this approximation diminishes as the required false-alarm rate goes to zero.

In this paper, we deal with the case where the parameters L and M are not small enough that a direct implementation of the exact distribution can be used, yet not large enough that the TW-derived methods are accurate. When the number of receivers is modest, in the range 2–5, we show that the calculation of a single threshold can be calculated accurately in only a few seconds using standard double-precision floating-

point arithmetic even when the number of samples is large, *i.e.*, $> 50\,000$.

In Section II, we introduce a simple signal model for a passive multistatic radar with a single transmitter and multiple surveillance-only receivers. The GCC statistic is introduced for the GLRT in Section III. In Section IV, the exact distribution function is presented along with its asymptotic approximation by the Tracy-Widom distribution. In Section V, the method to evaluate the distribution is presented. The new method is tested via numerical simulation on scenarios of different sizes in Section VI. Finally, receiver operating curves (ROC) are presented for the application to passive radar detection in order to demonstrate its practicality and superior accuracy.

II. SYSTEM MODEL

We consider a multistatic passive radar scenario with a single transmitter and M receivers. The possibility of a single target is considered which scatters the transmitted signal and is received at each of the receivers. The transmitted signal $s(t)$ is complex valued at baseband. The position of the transmitter, \mathbf{t} , and receivers, \mathbf{r}_m , are known whereas the presence of a target at position, \mathbf{p} , and velocity, \mathbf{v} , is not. In the received signals, the direct-path signal is assumed not to be present. That is, they are considered to be purely *surveillance signals*. In practice, this can be achieved by ensuring an antenna (or antenna array) null is steered towards the transmitter, or by blocking the direct-path intentionally with some other structure, natural or artificial.

If the target is present, the received signal therefore depends on the target position and velocity via two derived parameters, the time delay, τ_m , and frequency shift, ω_m . The delay, τ_m , is the time taken for the signal to travel between the transmitter and the m^{th} receiver via the target and has the value

$$\tau_m = \frac{1}{c}(\|\mathbf{p} - \mathbf{t}\| + \|\mathbf{p} - \mathbf{r}_m\|) \quad (1)$$

where c is the speed of light. Similarly, the frequency shift for a given velocity is the sum of the closing rates of the target to the transmitter and receiver, so that

$$\omega_m = \frac{\omega_0}{c} \mathbf{v}^T \left(\frac{\mathbf{p} - \mathbf{t}}{\|\mathbf{p} - \mathbf{t}\|} + \frac{\mathbf{p} - \mathbf{r}_m}{\|\mathbf{p} - \mathbf{r}_m\|} \right) \quad (2)$$

where ω_0 is the centre frequency of the transmitted signal. Hence, the m^{th} received signal has the form

$$x_m(t) = \mu_m s(t - \tau_m) e^{j\omega_m t} + \eta_m(t) \quad (3)$$

where μ_m represents the received amplitude, incorporating the effects of path length and target RCS, and $\eta_m(t)$ is receiver noise.

We wish to test the hypothesis that a target is present at the postulated position and velocity. Processing begins by correcting for the postulated delays τ_m and Doppler shifts ω_m so that when a target exists at that location,

$$\tilde{x}_m(t) = x_m(t + \tau_m) e^{-j\omega_m t} = \mu_m s(t) + \xi_m(t), \quad (4)$$

where $\xi_m(t)$ are the similarly modified noise components.

The received signals are sampled at an appropriate sampling frequency. L samples are used to form a vector $\tilde{\mathbf{x}}_m$ at each receiver. The modified noise $\xi_m(t)$ is also assumed to be additive white Gaussian noise and independent at each receiver. Likewise, \mathbf{s} is the vector of samples of $s(t)$ over the corresponding time interval.

The null hypothesis is that the received signal contains only noise

$$\mathcal{H}_0 : \tilde{\mathbf{x}}_m = \boldsymbol{\xi}_m. \quad (5)$$

Under the alternative hypothesis, there exists a target at position \mathbf{p} with velocity \mathbf{v} such that $\tilde{\mathbf{x}}_m$ has the form

$$\mathcal{H}_1 : \tilde{\mathbf{x}}_m = \mu_m \mathbf{s} + \boldsymbol{\xi}_m. \quad (6)$$

III. THE GCC STATISTIC AND THE GLRT

Formulating the likelihoods under each of the hypotheses and maximising the likelihood for the alternate hypothesis with respect to μ_m , we find [1] that the generalised (log) likelihood ratio is proportional to the largest eigenvalue, λ_1 , of the *Gram matrix*

$$\mathbf{G} = \boldsymbol{\Phi}^H \boldsymbol{\Phi}$$

where $\boldsymbol{\Phi} = (\tilde{\mathbf{x}}_1, \dots, \tilde{\mathbf{x}}_M)$ and the superscript H denotes the Hermitian transpose. The eigenvalue λ_1 is therefore a generalised likelihood ratio test (GLRT) statistic. Its similarity to a statistic originally proposed by Horst [12], [13] for generalised canonical correlation prompts us to refer to it as the ‘GCC’ statistic.

IV. EXPRESSIONS FOR THE DISTRIBUTION UNDER \mathcal{H}_0

Using the distribution of the GLRT statistic under the null hypothesis, a CFAR detector can be derived. In the case of \mathcal{H}_0 , the Gram matrix arises from a complex, central Wishart distribution. We will evaluate two approaches to modelling the distribution of this matrix’s largest eigenvalue: the exact expression of Kang & Alouini [11], denoted ‘KA’, and the asymptotic approximation that results from the distribution of Tracy & Widom [3], denoted ‘TW’.

We begin our treatment of detection thresholds by examining the approximation by the TW distribution. For complex samples, the distribution is Tracy-Widom of order 2 and the cumulative distribution function (c.d.f.) is denoted $F_2(x)$. El Karoui [14] showed that the true distribution of the largest eigenvalue, $F_{\lambda_1}(x)$, converges in a certain sense to $F_2(x)$ when L and M become large. Specifically, he found that

$$|F_{\lambda_1}(\tilde{\sigma}_{LM}x + \tilde{\mu}_{LM}) - F_2(x)| \leq C e^{-cx} L^{-2/3} \quad (7)$$

for constants C and c and sequences $\tilde{\mu}_{LM}$ and $\tilde{\sigma}_{LM}$ [15]. It is known that the right tail of $F_2(x)$ is of exponential order $\exp(-4x^{3/2}/3)$ [16]. Therefore, it can be seen that, for any fixed L and M , the error bound in (7) will overwhelm the tail probability as x becomes large.

The TW distribution is itself ‘‘somewhat tricky to compute numerically’’ [15]. In this paper, it’s calculated with the help of RMLab [17], which is a Matlab-based software package for the calculation of the TW distribution.

TABLE I
COMPUTATIONAL LIMITS IN DOUBLE-PRECISION FLOATING POINT
ARITHMETIC OF DIRECT IMPLEMENTATION OF THE KA EXPRESSION, (8).

Sensors (M)	Maximum samples (L)
2	98
3	71
4	57
5	47

The KA expression, on the other hand, is exact for finite L and M . For $L \geq M$ (the case of interest to us), it can be given in closed form as [11, Corollary 2]

$$F_{\lambda_1}(x) = \alpha \det \Psi(x) \quad (8)$$

where the elements of $\Psi(x)$ are defined as

$$\psi_{ij}(x) = \gamma(\tau + i + j - 1, x),$$

$\tau = L - M$, $\gamma(\cdot, \cdot)$ is the lower incomplete gamma function, which can be expressed as

$$\gamma(n, x) = (n-1)! \left(1 - e^{-x} \sum_{k=0}^{n-1} \frac{x^k}{k!} \right),$$

and

$$\alpha = \frac{1}{\prod_{m=1}^M (L-m)!(M-m)!}.$$

These expressions are well suited for direct numerical calculation only for small values of L and M . For larger values, the products of factorials quickly produce extremely large numbers and the sum term requires a large dynamic range to be accurately calculated. Depending on the number of receivers, the maximum number of samples is limited by the maximum value that can be represented in double-precision floating-point, *i.e.*, roughly 10^{308} . By using this upper bound, the number of samples is seen to be quickly limited as the number of sensors increases. A summary of these limits is shown in Table I.

V. HIGH-ACCURACY THRESHOLD CALCULATION

The primary objective in computing thresholds with high accuracy and over a wide range of L and M is to stave off floating-point overflow. It can be seen from (8) that the value of α quickly vanishes as L or M increases but at the same time the elements in $\Psi(x)$ become huge. We resist this tendency by regrouping terms.

First, we can decompose α so that

$$\alpha = \tilde{\alpha} \det \mathbf{D}^{-1} \det \mathbf{\Delta}^{-1}$$

We set

$$\mathbf{\Delta} = \text{diag}[(L-M)!, \dots, (L-1)!].$$

We entertain a choice for the remaining elements in the decomposition. Either we set

$$\tilde{\alpha} = \frac{1}{\prod_{m=1}^M (M-m)!} \quad \text{and} \quad \mathbf{D} = \mathbf{I} \quad (9)$$

or we set

$$\tilde{\alpha} = 1 \quad \text{and} \quad \mathbf{D} = \text{diag}[1, \dots, (M-1)!]. \quad (10)$$

For small values of M , say 2–5, and for $L \gg M$, it will become apparent that there's not much practical difference between these options. For larger values of M , the latter choice is to be preferred.

If we similarly decompose $\Psi(x)$ so that

$$\Psi(x) = \mathbf{D} \tilde{\Psi}(x) \mathbf{\Delta}$$

then it's clear that we can write

$$F_{\lambda_1}(x) = \tilde{\alpha} \det \tilde{\Psi}(x). \quad (11)$$

An alternative decomposition of $\Psi(x)$, in which the contribution of the incomplete gamma function is made explicit, is that

$$\Psi(x) = \mathbf{K} \circ [\mathbf{1} - \mathbf{Q}(x)] \quad (12)$$

where \mathbf{K} and $\mathbf{Q}(x)$ are $M \times M$ matrices defined with elements

$$k_{ij} = (\tau + i + j - 2)!$$

and

$$q_{ij}(x) = e^{-x} \sum_{k=0}^{\tau+i+j-2} \frac{x^k}{k!}, \quad (13)$$

$\mathbf{1}$ is the matrix of all 1s and the \circ operator represents the Hadamard (entry-wise) product.

Using an elementary, pseudo-commutative property of Hadamard products and diagonal matrices—see, for example, [18, Lemma 5.1.2]—(11) and (12) can be combined so that

$$F_{\lambda_1}(x) = \tilde{\alpha} \det \{ \tilde{\mathbf{K}} \circ [\mathbf{1} - \mathbf{Q}(x)] \} \quad (14)$$

where $\mathbf{K} = \mathbf{D} \tilde{\mathbf{K}} \mathbf{\Delta}$. According to our choice of (9) or (10), we consequently have the elements of $\tilde{\mathbf{K}}$ being

$$\tilde{k}_{ij} = \frac{(\tau + i + j - 2)!}{(\tau + j - 1)!} \quad \text{or} \quad \tilde{k}_{ij} = \frac{(\tau + i + j - 2)!}{(\tau + j - 1)!(i-1)!},$$

respectively.

Now consider the matrix $\mathbf{Q}(x)$. Observe from (13) that $0 \leq q_{ij}(x) \leq 1$ but that the terms evaluated within the sum can be very large. To avoid overflow, the e^{-x} term is moved inside the sum. The $x^k/k!$ term can also be large enough to cause overflow. Therefore, the summands are evaluated in the logarithm, *i.e.*, we write

$$q_{ij}(x) = \sum_{k=0}^{\tau+i+j-2} x^{\phi(x,k)} \quad (15)$$

where

$$\phi(x, k) = k - \frac{x + \log(k!)}{\log x}$$

and $\log(\cdot)$ denotes the natural logarithm.

We make two observations about speeding up the computation of $F_{\lambda_1}(x)$ as just described, under the assumption that many evaluations may be needed and for large values of x (corresponding to small values of false-alarm rate). First, at the expense of additional memory usage, the logarithms of the

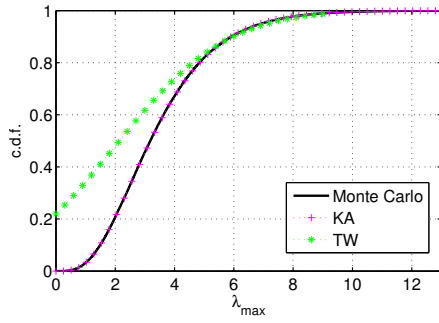


Fig. 1. Comparison of the theoretical (KA), empirical (Monte Carlo) and asymptotic (TW) c.d.f. for $L = M = 2$.

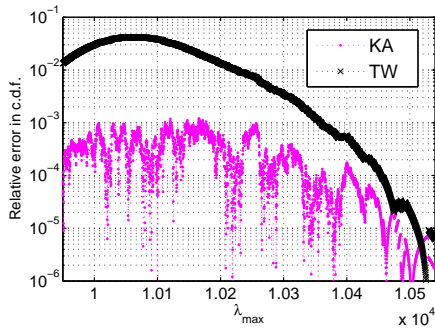


Fig. 2. Relative error of the c.d.f. computed using the KA expression and TW approximation compared to the empirical c.d.f. for $M = 2$ and $L = 10\,000$.

factorials can be pre-computed. Second, the summands in (15) should be computed from $k = \tau + i + j - 2$ down to $k = 0$, so that the summation can be halted early if the summands become insignificant.

VI. RESULTS

A. Accuracy of Distribution Expressions

We now evaluate the accuracy of the expressions for the distribution of the maximum eigenvalue. They are compared to results derived from 100 000 realisations of a Monte Carlo simulation of the null-hypothesis scenario. When the target is absent the received signal contains only noise. Accuracy is examined for sample size L varying from 2 to 10 000.

In Figure 1, the c.d.f. of the maximum eigenvalue, as evaluated using the KA expression, (8), is compared with the TW approximation, (7), and with the empirical c.d.f. obtained from Monte Carlo simulation. Here, $L = M = 2$ and the noise variance is set to one. The distribution is plotted over a wide range of values of λ_1 .

With a small number of samples and sensors, the closed-form KA expression for c.d.f. is simple to evaluate. The empirical c.d.f. shows good agreement. Meanwhile, the TW asymptotic approximation is visually close to the true c.d.f. for $x > 5$ but diverges noticeably for smaller values of x .

For scenarios that are more pertinent to passive radar, the new expression, (14), is used to evaluate the true (KA) c.d.f. Error relative to the empirical c.d.f. is presented in Figure 2

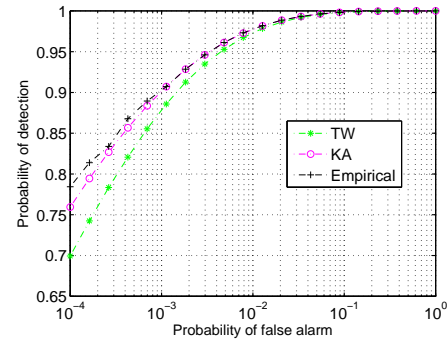


Fig. 3. ROC comparison of threshold-setting techniques for $M = 2$ and $L = 10\,000$ when a target is present at an SNR of -5 dB.

for $M = 2$ and $L = 10\,000$. Note that, because $L > 90$, the naïve implementation of KA would result in floating-point overflow. Compared to the $L = 2$ case, the accuracy of TW is much improved, though still clearly inferior to KA.

B. Application to Passive Radar

To further test the capabilities of the new KA expression in (14) and its applicability to passive radar, a receiver operating curve (ROC) is computed. We study a scenario where a target is present at a signal-to-noise ratio (SNR) of -5 dB.

Detection is performed using the GLRT. The threshold is set by three different techniques and the results compared. To test the TW approximation and the new KA expression, the threshold is set for an intended false-alarm rate (though, especially for TW, this may not correspond to the *realised* false-alarm rate). This is compared with a threshold that is set empirically from the Monte Carlo simulation used for Figure 2. By whatever means the threshold is set, the corresponding empirical detection probability is computed from a Monte Carlo simulation of 100 000 realisations.

The empirical probability of detection is plotted against the intended false-alarm rate in Figure 3. When the threshold is set using the TW approximation, we see that the detection probability is noticeably lower, by up to 5% over the range considered, when the intended false-alarm rate is below 10^{-2} . That is, there is a tendency with the TW approximation to set the threshold too high. On the other hand, good agreement is observed with the empirical data when the new KA expression is used to set the threshold.

VII. CONCLUSIONS

The computation of detection thresholds using the GLRT in multistatic passive radar with surveillance-only receivers is known to be computationally challenging. We have presented a practical technique for accurately computing false-alarm probabilities in standard double-precision floating-point arithmetic that enables a CFAR detector to be implemented. Through numerical simulations, we demonstrated that this approach yields a higher detection probability than is achieved when the Tracy-Widom distribution is used as an approximation.

REFERENCES

- [1] K. S. Bialkowski, I. V. L. Clarkson, and S. D. Howard, "Generalized canonical correlation for passive multistatic radar detection," in *IEEE Statistical Signal Processing Workshop (SSP)*, Nice, France, Jun. 2011, pp. 417–420.
- [2] D. Hack, L. Patton, B. Himed, and M. Saville, "Centralized passive MIMO radar detection without direct-path reference signals," *IEEE Transactions on Signal Processing*, vol. 62, no. 11, pp. 3013–3023, Jun. 2014.
- [3] C. A. Tracy and H. Widom, "Level-spacing distributions and the Airy kernel," *Physics Letters B*, vol. 305, no. 12, pp. 115–118, May 1993.
- [4] H. Griffiths and N. Long, "Television-based bistatic radar," *IEE Proceedings F, Communications, Radar and Signal Processing*, vol. 133, no. 7, pp. 649–657, Dec. 1986.
- [5] J. Palmer, D. Merrett, S. Palumbo, J. Piyaratna, S. Capon, and H. Hansen, "Illuminator of opportunity bistatic radar research at DSTO," in *IEEE Radar Conference*, Rome, Italy, Sep. 2008, pp. 701–705.
- [6] J. Palmer, S. Palumbo, T.-T. V. Cao, and S. Howard, "A new illuminator of opportunity bistatic radar research project at DSTO," Defence Science and Technology Organisation (Australia) Electronic Warfare and Radar Division, Tech. Rep., 2009.
- [7] P. Wang, H. Li, and B. Himed, "Moving target detection using distributed MIMO radar in clutter with nonhomogeneous power," *IEEE Transactions on Signal Processing*, vol. 59, no. 10, pp. 4809–4820, Oct. 2011.
- [8] A. M. Haimovich, R. S. Blum, and L. J. Cimini, "MIMO radar with widely separated antennas," *IEEE Signal Processing Magazine*, vol. 25, no. 1, pp. 116–129, 2008.
- [9] H. Gish and D. Cochran, "Generalized coherence [signal detection]," in *IEEE International Conference on Acoustics, Speech, and Signal Processing*, vol. 5, Apr. 1988, pp. 2745–2748.
- [10] K. Beudet, L. Crider, and D. Cochran, "Detection in networked radar," in *Algorithms for Synthetic Aperture Radar Imagery XX*, ser. Proc. SPIE, E. Zelnio and F. D. Garber, Eds., Apr. 2013, vol. 8746, pp. 87460V–1–9.
- [11] M. Kang and M.-S. Alouini, "Largest eigenvalue of complex Wishart matrices and performance analysis of MIMO MRC systems," *IEEE Journal on Selected Areas in Communications*, vol. 21, no. 3, pp. 418–426, 2003.
- [12] P. Horst, "Generalized canonical correlations and their application to experimental data," *Journal of Clinical Psychology*, vol. 17, no. 4, pp. 331–347, Oct. 1961.
- [13] J. R. Kettnering, "Canonical analysis of several sets of variables," *Biometrika*, vol. 58, no. 3, pp. 433–451, Dec. 1971.
- [14] N. El Karoui, "A rate of convergence result for the largest eigenvalue of complex white Wishart matrices," *The Annals of Probability*, vol. 34, no. 6, pp. 2077–2117, Nov. 2006.
- [15] I. M. Johnstone, "High dimensional statistical inference and random matrices," in *Proceedings of the International Congress of Mathematicians*, Aug. 2006, pp. 307–333.
- [16] J. Baik, R. Buckingham, and J. DiFranco, "Asymptotics of Tracy-Widom distributions and the total integral of a Painlevé II function," *Communications in Mathematical Physics*, vol. 280, no. 2, pp. 463–497, Feb. 2008.
- [17] M. Dieng, "RMLab, a MATLAB package for computing Tracy-Widom distributions and simulating random matrices." 2006. [Online]. Available: <http://math.arizona.edu/momar/research.htm>
- [18] R. A. Horn and C. R. Johnson, *Topics in Matrix Analysis*. Cambridge University Press, 1994.